

Equivalence of twistor prescriptions for super Yang–Mills

Sergei Gukov, Luboš Motl, and Andrew Neitzke

Jefferson Physical Laboratory, Harvard University, Cambridge,
MA 02138, USA

gukov@feynman.harvard.edu

motl@feynman.harvard.edu

neitzke@fas.harvard.edu

Abstract

There is evidence that one can compute tree-level super Yang–Mills amplitudes using either connected or completely disconnected curves in twistor space. We give a partial explanation of the equivalence between the two computations, by showing that they could both be reduced to the same integral over a moduli space of singular curves, subject to some assumptions about the choices of integration contours. We also formulate a class of new “intermediate” prescriptions to calculate the same amplitudes.

CONTENTS

1. Introduction	200
1.1. Notation and moduli spaces	204
2. Review of connected and disconnected prescriptions	205
2.1. Connected prescription	206
2.2. Disconnected prescription	208
3. Matching the prescriptions in degree 2 case	211
3.1. The argument in degree 2 case	211
3.2. Computing the residue in degree 2 case	212
3.3. Finishing the argument in degree 2 case	217
4. Higher degree	218
4.1. The proof in higher degree case	218
4.2. Intermediate prescriptions	220
4.3. Computing the residue in higher degree case	223
4.4. Finishing the argument in higher degree case	226
5. Conclusions and open questions	228
Acknowledgments	230
References	230

1 Introduction

Recently in [1], Witten proposed a new approach to perturbative gauge theories in four dimensions which, among other things, implies remarkable regularities in the perturbative scattering amplitudes of $\mathcal{N} = 4$ super Yang–Mills and leads to new ways of computing them. The scattering amplitudes in

question depend on the momentum and polarization vectors of the external gluons and are devilishly difficult to compute using the standard Feynman diagram techniques. For example, even computing a tree-level amplitude with four external gluons of positive helicity and three gluons of negative helicity (such an amplitude will be denoted $\mathcal{A}_{[++++---]}$) requires summing over hundreds of different diagrams!

According to the conjecture of [1], perturbative $\mathcal{N} = 4$ super Yang–Mills theory can be described as a string theory in twistor space $\mathbb{CP}^{3|4}$. In this reformulation, the Yang–Mills scattering amplitudes are given by certain integrals over moduli spaces of holomorphic curves in $\mathbb{CP}^{3|4}$, which can be interpreted as D1-brane instantons. More precisely, for a tree-level process involving q negative helicity gluons, the amplitude is given by an integral over moduli of curves of total degree d , where

$$d = q - 1. \tag{1.1}$$

For example, the simplest non-vanishing amplitude with $q = 2$ gluons of negative helicity¹ — the so-called maximally helicity violating (MHV) amplitude [2, 3] — can be computed by integrating over the moduli space of degree 1 curves in $\mathbb{CP}^{3|4}$ [1].

However, when one considers the next simplest case, $q = 3$, there is a puzzle. In the prescription of [1], this amplitude seems to involve a sum over two distinct contributions: one from an integral over connected degree 2 curves and another from an integral over disconnected pairs of degree 1 curves (figure 1). Surprisingly, in the case of $\mathcal{A}_{[+++---]}$, it was found that the contribution from connected degree 2 curves alone gives the full Yang–Mills amplitude, at least up to a multiplicative constant [4]. This computation was extended to all googly [5] and some non-MHV [6] amplitudes, again with the surprising result that connected degree d curves already account for the full Yang–Mills amplitude, without adding any disconnected curves.

On the other hand, there is some evidence that these tree-level amplitudes can also be computed by considering only the contribution of curves which are “maximally disconnected,” namely, they consist of d distinct degree 1 lines. Since degree 1 curves are associated with MHV amplitudes, this result suggests an alternative method of computing generic tree amplitudes from graphs with MHV vertices [7]. The number v of vertices is determined by the

¹We follow the conventions of [1] where an n -gluon scattering amplitude is called MHV if $n - 2$ external gluons have positive helicity, and $\overline{\text{MHV}}$ (or “googly”) if $n - 2$ gluons have negative helicity.

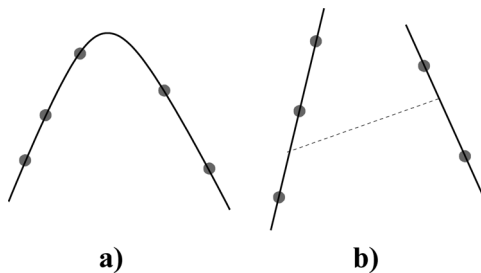


Figure 1: An instanton contribution: (a) from a connected curve of degree 2; (b) from a pair of degree 1 curves. The dotted line represents a propagator in holomorphic Chern–Simons theory.

number of gluons with negative helicity; it is actually equal to degree (1.1),

$$v = q - 1. \quad (1.2)$$

This approach leads to a spectacular simplification of the computations. For example, the 7-gluon amplitude $\mathcal{A}_{[++++----]}$ mentioned earlier can be computed using only eight diagrams with MHV vertices. However, it also leads to a puzzle.

As we just discussed, the evidence so far in the literature suggests that rather than one prescription for Yang–Mills amplitudes there are at least two: one involving connected curves only and another involving maximally disconnected ones. We will refer to these as the “connected prescription” and the “disconnected prescription,” respectively. These different prescriptions have so far not been related directly. In a sense, they seem to have complementary virtues: the connected prescription expresses the whole amplitude as a single integral, and from this form it is easier to prove some properties of the amplitude, such as the parity symmetry; on the other hand, the disconnected prescription leads to concrete and immediately useful formulas for the tree-level amplitudes.

The purpose of this note is to provide a partial explanation of why the connected and disconnected prescriptions are equivalent. The explanation is that, in both prescriptions, the integrand on the moduli space has a pole on a submoduli space parameterizing configurations of intersecting degree 1 curves. Moreover, the residue of the integrand at this pole is the same in both cases. So if the integrals over the moduli spaces both localize to this same pole, e.g., by a residue formula, it would lead to a natural proof of the equivalence between the two prescriptions. We emphasize that the arguments of this paper do not constitute a complete proof of the equivalence; we identify the necessary poles, but do not specify precisely the contour of integration to be chosen in either prescription.

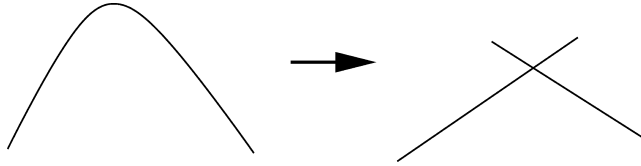


Figure 2: A curve of degree 2 can degenerate into a pair of intersecting lines.

Let us illustrate this explanation in the simplest case of degree 2 curves (figure 2). We have two different moduli spaces, $\overline{\mathcal{M}}_{0,n,2}$ and $\mathcal{M}_{\text{lines}}$, parameterizing, respectively, connected degree 2 curves in $\mathbb{CP}^{3|4}$ and disconnected pairs of lines in $\mathbb{CP}^{3|4}$, and integrands ω_{conn} and ω_{disc} on the two spaces (we will review the construction of these integrands in Section 2). Our job is to explain the equality

$$\int_{\overline{\mathcal{M}}_{0,n,2}} \omega_{\text{conn}} = \int_{\mathcal{M}_{\text{lines}}} \omega_{\text{disc}}. \quad (1.3)$$

The explanation begins by noting that both $\mathcal{M}_{\text{lines}}$ and $\overline{\mathcal{M}}_{0,n,2}$ contain a codimension-1 “degeneration locus” \mathcal{M}_{int} parameterizing the moduli of pairs of intersecting lines in $\mathbb{CP}^{3|4}$. In the case of $\mathcal{M}_{\text{lines}}$, we get such a degenerate configuration just by taking two lines in $\mathbb{CP}^{3|4}$ which happen to intersect. For $\overline{\mathcal{M}}_{0,n,2}$, we get such a degeneration by considering a hyperbola $xy = C$ in the limit $C \rightarrow 0$, appropriately embedded in $\mathbb{CP}^{3|4}$. The crucial point is that both ω_{conn} and ω_{disc} turn out to have a simple pole along \mathcal{M}_{int} , and furthermore the residue is the same in both cases.² Therefore, provided that the integration contours on $\mathcal{M}_{\text{lines}}$ and $\overline{\mathcal{M}}_{0,n,2}$ are chosen compatibly (so that they both encircle \mathcal{M}_{int} and reduce to the same contour along it), the desired agreement follows.

The argument for general degree d proceeds along similar lines. In the moduli space $\overline{\mathcal{M}}_{0,n,d}$, we find a pole where a degree d curve degenerates into two intersecting curves of degrees d_1 and d_2 ; the integral over $\overline{\mathcal{M}}_{0,n,d}$ localizes to this sublocus, then inside this sublocus, there is a pole where one of the two curves degenerates further, and so on until we reduce finally to the moduli space \mathcal{M}_{int} of connected trees built from degree 1 curves. On the other hand, the integral over $\mathcal{M}_{\text{lines}}$ also reduces to the same \mathcal{M}_{int} , because the propagators connecting the different lines have poles when the lines intersect. Furthermore, it turns out that the integrands on \mathcal{M}_{int} coming from the two prescriptions are proportional. This establishes the agreement between these two prescriptions, again provided that the contours can be chosen appropriately, and up to an overall constant which we do not fix.

²We learned of the possibility of such an explanation from Edward Witten.

This iterative argument pays a surprising dividend: for any $K = 0, \dots, d - 1$, we can define an “intermediate prescription,” in which we integrate over configurations of $K + 1$ curves with total degree d . We will show that all of these intermediate prescriptions agree with the connected and disconnected prescriptions. They can also be understood diagrammatically: one sums over tree diagrams with $K + 1$ vertices, where each vertex is decorated with a degree. In these notations, vertices of degree 1 are the MHV vertices of [7], whereas vertices with $d > 1$ could be called “non-MHV vertices.” These intermediate prescriptions deserve further study.

For other recent work on the twistor string approach to Yang–Mills, see [4–6, 8–10] for the connected prescription, [7, 11, 12] for the disconnected prescription, and [13–15] for related topics.

1.1 Notation and moduli spaces

We always consider scattering amplitudes of n external gluons associated with the particular trace factor $\text{Tr}(T_1 T_2 \cdots T_n)$.

We use a coordinate representation for the super twistor space $\mathbb{C}^{4|4}$. We unify the bosonic and fermionic indices into a superspace index \mathbb{A} taking values in

$$\mathbb{A} \in \{1, 2, 3, 4 | 1', 2', 3', 4'\}. \quad (1.4)$$

The components of all objects with bosonic values of the superspace index are commuting, while components with fermionic (primed) values of the superspace index are anticommuting. The coordinates on the super twistor space will be denoted by $Z^{\mathbb{A}}$, which are related to the coordinates in the literature by

$$(Z^1, Z^2, Z^3, Z^4 | Z^{1'}, Z^{2'}, Z^{3'}, Z^{4'}) = (\lambda^1, \lambda^2, \mu^1, \mu^2 | \psi^1, \psi^2, \psi^3, \psi^4) \in \mathbb{C}^{4|4}. \quad (1.5)$$

We will also be considering various moduli spaces of curves in $\mathbb{C}\mathbb{P}^{3|4}$ with marked points. We use the standard notation

$$\mathcal{M}_{0,n,d}(\mathbb{C}\mathbb{P}^{3|4}) \quad (1.6)$$

for the moduli space of “genus 0, n -pointed curves of degree d in $\mathbb{C}\mathbb{P}^{3|4}$.” This moduli space has dimension $(4d + n)|(4d + 4)$. As in [1], we realize it as the space of automorphism classes of maps $\mathbb{C}\mathbb{P}^1 \rightarrow \mathbb{C}\mathbb{P}^{3|4}$, of degree d , with n marked points on $\mathbb{C}\mathbb{P}^1$. Since the target space is always $\mathbb{C}\mathbb{P}^{3|4}$ in this paper, sometimes we abuse notation and write simply $\mathcal{M}_{0,n,d}$.

We will be interested in integrating over $\mathcal{M}_{0,n,d}(\mathbb{CP}^{3|4})$, so we need to understand the properties of this moduli space. First, $\mathcal{M}_{0,n,d}(\mathbb{CP}^{3|4})$ is non-compact, due to certain degenerations that a degree d curve with n marked points can have which are not simply described by a map $\mathbb{CP}^1 \rightarrow \mathbb{CP}^{3|4}$. One type of degeneration that will be important below is when a curve develops a node, i.e., splits into two components. There is a standard way of incorporating these degenerate curves into our moduli space of maps; one then obtains a larger compact space $\overline{\mathcal{M}}_{0,n,d}(\mathbb{CP}^{3|4})$, called the “moduli space of stable maps.” This moduli space is a smooth algebraic variety, except for certain orbifold points which will not play an important role in this paper.³

In particular, the “boundary” of this moduli space,

$$\overline{\mathcal{M}}_{0,n,d}(\mathbb{CP}^{3|4}) \setminus \mathcal{M}_{0,n,d}(\mathbb{CP}^{3|4}), \quad (1.7)$$

contains a codimension 1 divisor which parameterizes curves which have split into two components. Similarly, for any K , there is a subspace $\mathcal{M}_{\text{int}}^K$ of codimension K that parameterizes reducible curves with K nodes, i.e., curves which have split up into $K+1$ intersecting components which intersect in a tree. This $\mathcal{M}_{\text{int}}^K$ can be further decomposed into irreducible pieces,

$$\mathcal{M}_{\text{int}} = \bigcup_{\Gamma} \mathcal{M}_{\text{int}}^{\Gamma}, \quad (1.8)$$

where the different Γ label different shapes of the tree, together with different decompositions of d into individual degrees $\{d_i\}$, $i = 1, 2, \dots, K+1$, $d_i \geq d_{i+1}$, and different ways in which the n marked points can be distributed over the $K+1$ components. Some of these $\mathcal{M}_{\text{int}}^{\Gamma}$ will play an important role in our discussion below.

2 Review of connected and disconnected prescriptions

Suppose we want to use the twistor prescription of [1] to evaluate a Yang–Mills amplitude with $q = d + 1$ negative helicity gluons. All contributions to this amplitude are expected to involve holomorphic curves of total degree d , but a priori these can be either connected or disconnected. In this section we review the contributions which would be expected from the two most extreme cases: connected degree d curves and completely disconnected families of d degree 1 curves.

³Strictly speaking, this theorem has been proven when the target space is \mathbb{CP}^3 [16], not for the supermanifold $\mathbb{CP}^{3|4}$, but we do not expect any important differences.

In both cases we will consider the Yang–Mills amplitude with arbitrary external scattering states. Via the Penrose transform these scattering states are described by twistor space wavefunctions,⁴ which are $\bar{\partial}$ -closed $(0, 1)$ forms ϕ_i ($i = 1, \dots, n$) on $\mathbb{CP}^{3|4}$. We always treat these ϕ_i as generic. In our computation, we will be focusing on poles which arise in integrals over moduli spaces of curves; we emphasize that the poles in question never come from the ϕ_i .

The prescriptions as we write them below are not gauge-invariant. To make the amplitudes gauge-invariant, we would probably have to include additional diagrams in both prescriptions, involving cubic Chern–Simons interaction vertices. Nevertheless, both prescriptions make sense provided we choose a specific gauge for the gauge field, such as an axial gauge. In this gauge, one expects that the cubic vertices do not contribute [1].⁵

2.1 Connected prescription

We first review the connected prescription for computation of n -point Yang–Mills amplitudes. The amplitude is obtained as an integral over degree d maps

$$P: \mathbb{CP}^1 \rightarrow \mathbb{CP}^{3|4}. \tag{2.1}$$

Such a map P can be written explicitly, in terms of the inhomogeneous coordinate σ on \mathbb{CP}^1 , as

$$P^\mathbb{A}(\sigma) = Z^\mathbb{A} = \sum_{k=0}^d \beta_k^\mathbb{A} \sigma^k \tag{2.2}$$

The supermoduli of the degree d map P are $\beta_k^\mathbb{A}$; these span a space $\mathbb{C}^{4d+4|4d+4}$, which comes equipped with the natural measure

$$\mu_d = \prod_{k,\mathbb{A}} d\beta_k^\mathbb{A}. \tag{2.3}$$

We also have a holomorphic n -form on $(\mathbb{CP}^1)^n$ given by the free-fermion correlator,

$$\omega(\sigma_1, \dots, \sigma_n) = \prod_{i=1}^n \frac{d\sigma_i}{\sigma_i - \sigma_{i+1}}, \quad \sigma_{n+1} \equiv \sigma_1. \tag{2.4}$$

⁴Actually, the wave functions are not defined on all of $\mathbb{CP}^{3|4}$, but this distinction will not be important for us.

⁵We thank Peter Svrček for reminding us of this point.

Note that both μ and ω are invariant under the group $GL(2, \mathbb{C})$ that acts linearly on the homogeneous coordinates on $\mathbb{C}P^1$. Its action on σ is given by the usual expression

$$\sigma \mapsto \sigma' = \frac{a\sigma + b}{c\sigma + d}, \quad ad - bc \neq 0 \quad (2.5)$$

while its action on $\beta_k^\mathbb{A}$ is dictated by the invariance of $Z^\mathbb{A}$ in (2.2): the coefficients $\beta_k^\mathbb{A}$ may be re-organized (up to some combinatorial factors suppressed for simplicity) into a rank d tensor under $GL(2, \mathbb{C})$,

$$\{\beta_k^\mathbb{A}\} = \{\beta_{I_1 I_2 \dots I_d}^\mathbb{A}\}, \quad I_l = 1, 2, \quad (2.6)$$

where the number of indices $I_l = 2$ equals k , so that the action of $GL(2, \mathbb{C})$ on $\beta_k^\mathbb{A}$ becomes

$$\beta_{I_1 I_2 \dots I_d}^\mathbb{A} \mapsto \beta'_{I_1 I_2 \dots I_d}^\mathbb{A} = M_{I_1}^{I'_1} M_{I_2}^{I'_2} \dots M_{I_d}^{I'_d} \beta_{I'_1 I'_2 \dots I'_d}^\mathbb{A}, \quad M_I^{I'} = \begin{pmatrix} d & -b \\ -c & a \end{pmatrix}. \quad (2.7)$$

Along with μ and ω , we also have to include the external wave functions,⁶

$$\Phi = \prod_{i=1}^n \phi_i(P(\sigma_i)). \quad (2.8)$$

Putting everything together, the Yang–Mills amplitude is formally⁷

$$\int_{\overline{\mathcal{M}_{0,n,d}}} \frac{\mu_d \wedge \omega(\sigma_1, \dots, \sigma_n)}{\text{vol}(GL(2, \mathbb{C}))} \wedge \Phi. \quad (2.9)$$

Expression (2.9) is formal for several reasons. The first and most serious reason is that we have to choose a contour for the integral over the coordinates $\beta_k^\mathbb{A}$ in $\overline{\mathcal{M}_{0,n,d}}$, and the proper choice of contour is not yet well understood. (We do not have to choose a contour for the integrals over σ , because the integrand includes both $d\sigma$ from ω and $d\bar{\sigma}$ from the external wave functions). We will have more to say about the contour below; to match the disconnected prescription, we will essentially use a contour around infinity (suitably defined) so that *all* residues are counted.

Second, we have to divide out by the action of $GL(2, \mathbb{C})$. A convenient gauge-fixing will be chosen below, but of course the amplitude is independent of the choice of gauge. We should perhaps mention that we consider

⁶We write $\phi(P(\sigma_i))$ for the pullback of ϕ to moduli space via the evaluation map sending P to $P(\sigma_i)$.

⁷Here and below, by $\text{vol}(GL(2, \mathbb{C}))$, we really mean the volume form on that group; this is just the standard quotient, when written in terms of an integral over the quotient space.

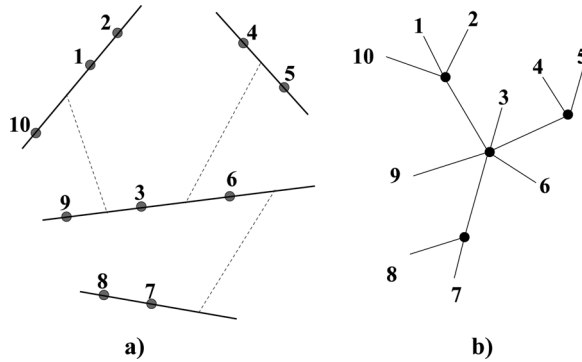


Figure 3: A contribution to Yang–Mills amplitudes with five positive and five negative helicity gluons, represented (a) as four disconnected lines in twistor space, (b) as a graph Γ with four MHV vertices.

$GL(2, \mathbb{C})$ over \mathbb{C} , i.e., we divide by the “holomorphic” volume form. This means that

- this symmetry will always be fixed by a set of holomorphic conditions;
- we will sum over all inequivalent solutions;
- only the holomorphic Jacobian will be included in the integrals.

These rules are compatible with the computations of [4–6].

2.2 Disconnected prescription

Now we describe the disconnected prescription for the same amplitudes, formulated in twistor space along the lines of the derivation given in [7]. In this prescription, a tree-level amplitude involving $d + 1$ negative helicity gluons, with a particular cyclic ordering, is obtained as a sum over various tree diagrams with d vertices. In figure 3, we show a representative example of a diagram Γ which contributes to amplitudes with five positive and five negative helicity gluons. The 10 external gluons are arranged cyclically around the index loop, and since there are five negative helicity gluons there are $5 - 1 = 4$ vertices. The vertices have arbitrary valence.⁸ We have not specified which gluons have which helicities; the twistor space computation yields superspace expressions which generate the answers for all possible choices when suitably expanded in the fermionic coordinates (figure 4).

⁸Ultimately, it turns out that any diagram containing a vertex of valence ≤ 2 does not contribute to the amplitude [7].

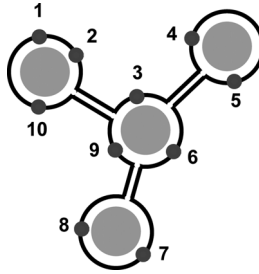


Figure 4: A different version of figure 3, representing the same single-trace amplitude with the index line made manifest. The circles represent degree 1 curves in twistor space.

Each vertex of Γ corresponds to a \mathbb{CP}^1 in $\mathbb{CP}^{3|4}$, equipped with marked points corresponding to internal or external lines attached to the vertex. To compute the contribution of Γ to the amplitude, we have to integrate over the moduli of these curves, given by d degree 1 maps

$$Q_i: \mathbb{CP}^1 \rightarrow \mathbb{CP}^{3|4}. \quad (2.10)$$

Each such map can be written

$$Q_i^{\mathbb{A}}(\sigma) = \sum_{k=0}^1 \beta_{k,i}^{\mathbb{A}} \sigma^k \quad (2.11)$$

so there are a total of $8d|8d$ supermoduli $\beta_{k,i}^{\mathbb{A}}$ for these d maps, reduced to $4d|8d$ by the $GL(2, \mathbb{C})^d$ symmetry. We also have to integrate over the moduli for the marked points; if in the diagram Γ there are n_i marked points on the i -th \mathbb{CP}^1 , then the full moduli space is

$$\mathcal{M}_{\text{lines}}^{\Gamma} = \prod_{i=1}^d \mathcal{M}_{0,n_i,1}(\mathbb{CP}^{3|4}). \quad (2.12)$$

As in the connected case, there is a natural measure for the moduli of the curves,

$$\mu_{\text{lines}} = \prod_{k,\mathbb{A},i} d\beta_{k,i}^{\mathbb{A}}. \quad (2.13)$$

There are several factors in the integrand which depend on the marked points. First, there is a free-fermion correlator for each curve; the points on the i th \mathbb{CP}^1 come with a cyclic ordering as indicated in figure 3, and if we label them $\sigma_1, \dots, \sigma_{n_i}$, they contribute

$$\omega_i = \omega(\sigma_1, \dots, \sigma_{n_i}) \quad (2.14)$$

with ω defined in (2.4). These free-fermion correlators contain $d\sigma$ for each marked point.

Next we have to include the external wave functions: each external wave function ϕ_j is connected to a marked point σ on the i th \mathbb{CP}^1 , for some i , and the integrand includes the factor

$$\phi_j(Q_i(\sigma)) \tag{2.15}$$

just as in the connected prescription. But unlike the connected prescription, here we also have some marked points which are connected to internal propagators. Let us write $D(\cdot, \cdot)$ for the twistor space propagator, which is a $(0, 2)$ -form on $\mathbb{CP}^{3|4} \times \mathbb{CP}^{3|4}$. Each internal propagator is connected to two marked points σ, σ' on the i th and i' th \mathbb{CP}^1 's, respectively, for some i, i' , and contributes to the integrand a factor

$$D(Q_i(\sigma), Q_{i'}(\sigma')). \tag{2.16}$$

Let us write $\Phi \wedge D$ for the product of all the wave functions and propagators from (2.15) and (2.16). Since every marked point is attached either to a propagator or to an external wave function, this $\Phi \wedge D$ includes one factor $d\bar{\sigma}$ for each marked point.

Then the amplitude in the disconnected prescription is given by the sum over tree diagrams,

$$\sum_{\Gamma} \int_{\mathcal{M}_{\text{lines}}^{\Gamma}} \frac{\mu_{\text{lines}} \wedge \left(\prod_{i=1}^d \omega_i \right) \wedge \Phi \wedge D}{\text{vol}(GL(2, \mathbb{C}))^d}. \tag{2.17}$$

As with the connected prescription, to make this integral concrete, we have to do two more things. First, we must gauge-fix the symmetry $GL(2, \mathbb{C})^d$ which acts separately on each \mathbb{CP}^1 . Second, we must choose a contour for the integrals over the moduli $\beta_{k,i}^{\mathbb{A}}$.

In [7], it was argued that if one makes a particular choice of contour, and chooses external wave functions corresponding to gluons of fixed helicity and momentum, then the integral over $\mathcal{M}_{\text{lines}}^{\Gamma}$ in (2.17) can be evaluated by a simple rule. Namely, one first assigns $(+)$ and $(-)$ helicities to the endpoints of each propagator, consistent with the rule that each vertex should have exactly two $(-)$ helicities on it; for given Γ , there is at most one way to do this. (If there is no way to do it, then the diagram Γ just contributes zero). Then each vertex gives a copy of the MHV amplitude — continued off-shell in a specific way to accommodate the internal lines — while each propagator carrying momentum q gives $1/q^2$.

For future use in Section 4.2, we also mention a natural generalization of the disconnected prescription: instead of using d degree 1 curves, we could use $K + 1$ curves for some K , with total degree d , connected into a tree by K propagators. The integrand is then defined in a way precisely analogous

to (2.17), except that the sum over Γ includes all choices for the degrees of the curves in addition to distributions of the marked points.

3 Matching the prescriptions in degree 2 case

3.1 The argument in degree 2 case

How can the disconnected and connected prescriptions give the same result? Let us consider next-to-MHV amplitudes, $q = 3$, which come from degree 2 curves. We postpone the discussion of curves of higher degree to Section 4.

The contribution of disconnected instantons comes from pairs of degree 1 curves connected by a single propagator, with n marked points distributed over the pair of curves. This moduli space has dimension $(8 + n)|16$ (which includes $4|8$ for each degree 1 curve plus n for the marked points). Different distributions of the marked points correspond to different MHV diagrams Γ .⁹

It was shown in [7] that for each Γ the integrand in (2.17) has a simple pole on the submoduli space $\mathcal{M}_{\text{int}}^\Gamma$, parameterizing degenerate configurations of intersecting lines of degree 1. This submoduli space has dimension $(7 + n)|12$, because the condition that there exists an intersection in the bosonic space removes one bosonic modulus, and the condition that all four fermionic coordinates of the two lines coincide at this point removes four fermionic moduli.¹⁰

After contour-integrating to localize to $\mathcal{M}_{\text{int}}^\Gamma$, the sum (2.17) can be written as

$$\sum_{\Gamma} \int_{\mathcal{M}_{\text{int}}^\Gamma} \frac{1}{\text{vol}(GL(2, \mathbb{C}))^2} \left(\mu_{\text{int}} \wedge \left(\prod_{i=1}^{n_1} \frac{d\sigma_i}{\sigma_i - \sigma_{i+1}} \right) \wedge \left(\prod_{j=1}^{n_2} \frac{d\sigma'_j}{\sigma'_j - \sigma'_{j+1}} \right) \right) \wedge \Phi. \quad (3.1)$$

Here i and j run over the marked points on each \mathbb{CP}^1 , including the point of intersection; so for a diagram with m external wave functions attached

⁹There are $n(n+1)/2$ such diagrams, although once we fix the external wave functions not every diagram gives a non-zero contribution to the sum (2.17); if the helicities are $- - - + + + \cdots + +$, then there are $2(n-3)$ diagrams which contribute.

¹⁰This fermionic delta function guarantees the opposite helicity of the two endpoints of the propagators when one expands in fermions to evaluate a particular amplitude.

to the first line, $n_1 = m + 1$ and $n_2 = n - m + 1$. Also, $\sigma_{n_1+1} \equiv \sigma_1$ and $\sigma'_{n_2+1} \equiv \sigma'_1$. The measure μ_{int} is completely determined by the symmetries of $\mathbb{CP}^{3|4}$.

On the other hand, from the connected prescription (2.9), we find

$$\int_{\overline{\mathcal{M}}_{0,n,2}} \frac{1}{\text{vol}(GL(2, \mathbb{C}))} \left(\mu_2 \wedge \left(\prod_{i=1}^n \frac{d\sigma_i}{\sigma_i - \sigma_{i+1}} \right) \right) \wedge \Phi. \quad (3.2)$$

We will re-organize integral (3.2) over the $(8+n)|12$ -dimensional space $\overline{\mathcal{M}}_{0,n,2}$ of conics in the following way: locally, to any conic we will associate a pair of intersecting lines which are its “asymptotes.” The moduli space of pairs of intersecting lines with n marked points is the \mathcal{M}_{int} which occurred in the disconnected prescription. This \mathcal{M}_{int} has dimension $(7+n)|12$, so in $\overline{\mathcal{M}}_{0,n,2}$, there is one more coordinate, which we call C ; $C = 0$ corresponds to the singular conics, which coincide with their asymptotes. This C can be thought of as a “deformation parameter” which resolves the singularity. We will find that the integrand has a pole at $C = 0$, i.e., along \mathcal{M}_{int} .

More precisely, \mathcal{M}_{int} includes only those degenerations in which the marked points are distributed in a way corresponding to some MHV tree graph Γ . This just means the points are broken into two groups which are cyclically ordered — so, e.g., if $n = 6$, there is a component of \mathcal{M}_{int} with points 1, 2, 3 on one line and 4, 5, 6 on the other, but we do not include the degeneration which has 1, 2, 4 on one line and 3, 5, 6 on the other. Indeed, we will see that the latter degeneration does *not* give a pole. We will find poles only along $n(n+1)/2$ distinct components $\mathcal{M}_{\text{int}}^\Gamma$, which are in one-to-one correspondence with the diagrams Γ contributing to (3.1).

Moreover, we will show that the residue along $\mathcal{M}_{\text{int}}^\Gamma$ is precisely such that the integral (3.2) agrees with (3.1) after localizing. This will complete the argument for the equivalence in the degree 2 case.

3.2 Computing the residue in degree 2 case

In this section, we show that integral (3.2) over the moduli space $\overline{\mathcal{M}}_{0,n,2}$ of genus zero, degree 2 curves in $\mathbb{CP}^{3|4}$ with n marked points has a pole at the subspace \mathcal{M}_{int} describing pairs of intersecting lines, and that it has the desired residue as discussed in the last section.

Let us start by fixing part of the $GL(2, \mathbb{C})$ symmetry reviewed in Section 2.1. We use three generators of $GL(2, \mathbb{C})$ to impose the constraints

$$P^4(\sigma) = \sigma \quad \text{i.e.} \quad (\beta_0^4, \beta_1^4, \beta_2^4) = (0, 1, 0). \quad (3.3)$$

In other words, we are imposing the conditions that the two intersections of the hyperplane $Z^4=0$ with the curve have coordinates¹¹ $\sigma = 0$ and $\sigma = \infty$ and normalizing the coefficients $\beta_{0,1,2}^4$. There is one more generator of $GL(2, \mathbb{C})$ to be fixed, the matrix

$$M = \begin{pmatrix} \lambda & 0 \\ 0 & \lambda^{-1} \end{pmatrix}, \quad (3.4)$$

which acts as

$$\beta_k^\mathbb{A} \rightarrow \lambda^{2-2k} \beta_k^\mathbb{A}, \quad \sigma \rightarrow \lambda^2 \sigma. \quad (3.5)$$

This transformation preserves the gauge choice (3.3).

3.2.1 Factors from the measure on the moduli space

Using the freedom to divide all twistor coordinates $Z^\mathbb{A}$ by σ , we can write (2.2) as

$$P^\mathbb{A}(\sigma) = Z^\mathbb{A} = \sum_{k=0}^2 \beta_k^\mathbb{A} \sigma^{k-1} = \beta_0^\mathbb{A} \sigma^{-1} + \beta_1^\mathbb{A} + \beta_2^\mathbb{A} \sigma, \quad (3.6)$$

which using (3.3) implies $P^4(\sigma) = 1$. As $\sigma \rightarrow \infty$ or $\sigma \rightarrow 0$, we can neglect the first or the last term in (3.6), respectively. So (3.6) describes a hyperbola that approaches two asymptotic lines in the superspace $\mathbb{C}^{3|4}$:

$$Z^\mathbb{A} = \beta_0^\mathbb{A} \sigma^{-1} + \beta_1^\mathbb{A}, \quad Z^\mathbb{A} = \beta_1^\mathbb{A} + \beta_2^\mathbb{A} \sigma. \quad (3.7)$$

These two lines intersect at the point $Z^\mathbb{A} = \beta_1^\mathbb{A}$, while $\beta_0^\mathbb{A}$ and $\beta_2^\mathbb{A}$ with $\mathbb{A} \neq 4$ are the tangent vectors along these lines. It is important that for every conic $\Sigma := P_*(\mathbb{C}\mathbb{P}^1) \subset \mathbb{C}\mathbb{P}^{3|4}$ we can find a singular conic Σ' (a pair of intersecting lines) in \mathcal{M}_{int} defining the asymptotes of Σ . This rule is not canonical; it depended on our choice to single out the points at infinity, i.e., the hyperplane $Z^4=0$.

We want to express $\overline{\mathcal{M}_{0,n,2}}$ locally as a product of \mathcal{M}_{int} and \mathbb{C} , with the extra \mathbb{C} parameterized by the deformation parameter C . What are the appropriate coordinates? The 3|4 parameters

$$\beta_1^\mathbb{A}, \quad \mathbb{A} \neq 4, \quad (3.8)$$

describing the position of the intersection of the asymptotes, give coordinates on \mathcal{M}_{int} . The remaining 4|8 coordinates on \mathcal{M}_{int} are the directions of the two asymptotes; each asymptote gives us 2|4 moduli. We want to describe these directions by “unit vectors” in a suitable sense. As we approach a generic point of \mathcal{M}_{int} , β_0^3 and β_2^3 are non-zero, and we may use them to

¹¹The point $\sigma = \infty$ can be written as (1:0) in homogeneous coordinates, and therefore is completely non-singular.

normalize the direction vectors. In other words, the remaining 2|4 plus 2|4 coordinates on \mathcal{M}_{int} may be chosen as

$$\frac{\beta_0^{\mathbb{A}}}{\beta_0^3} \text{ and } \frac{\beta_2^{\mathbb{A}}}{\beta_2^3}, \quad \mathbb{A} \in \{1, 2|1', 2', 3', 4'\}. \tag{3.9}$$

(Choosing different coordinates on \mathcal{M}_{int} instead of (3.8) and (3.9) would not change the result below; the only change would be a C -independent Jacobian).

Looking at our original coordinates on $\overline{\mathcal{M}_{0,n,2}}$, we still have two more bosonic components of β which are independent of our coordinates on \mathcal{M}_{int} , namely β_0^3 and β_2^3 themselves. We also have one unfixed generator of $GL(2, \mathbb{C})$ given in (3.5). This generator simply multiplies the ratio β_0^3/β_2^3 by λ^4 , so we can use it to fix that ratio to a constant, such as

$$\frac{\beta_0^3}{\beta_2^3} = 1. \tag{3.10}$$

Now having fixed the full $GL(2, \mathbb{C})$ symmetry, we can write the measure μ_2 from (2.3) as

$$\left(\frac{J}{4}\right) \prod_{k,\mathbb{A}} d\beta_k^{\mathbb{A}} \delta\left(\frac{\beta_0^3}{\beta_2^3 - 1}\right) \delta(\beta_0^4) \delta(\beta_1^4 - 1) \delta(\beta_2^4). \tag{3.11}$$

Here J is the determinant of the Jacobian matrix of variations of the constraints with respect to the $GL(2, \mathbb{C})$ generators. If we parameterize the generators of $GL(2, \mathbb{C})$ by

$$M = \begin{pmatrix} 1 + a & b \\ c & 1 + d \end{pmatrix} \tag{3.12}$$

then this matrix is

$$\delta \begin{pmatrix} \beta_0^4 \\ \beta_1^4 \\ \beta_2^4 \\ \beta_0^3/\beta_2^3 \end{pmatrix} = \begin{pmatrix} 1 & 0 & 0 & 0 \\ 0 & 1 & 0 & 0 \\ 0 & 0 & 1 & 1 \\ * & * & 2 & -2 \end{pmatrix} \begin{pmatrix} b \\ c \\ a \\ d \end{pmatrix} \tag{3.13}$$

and hence we get simply

$$J = -4. \tag{3.14}$$

The factor $J/4$ in (3.11) represents $1/\text{vol}(GL(2, \mathbb{C}))$; we had to divide by 4 because the $\mathbb{Z}_4 \subset GL(2, \mathbb{C})$ generated by

$$M = \begin{pmatrix} i & 0 \\ 0 & -i \end{pmatrix} \tag{3.15}$$

is left unfixed by our gauge condition.

The three delta functions in (3.11) involving β_k^4 just eliminate the integrals over those variables, imposing (3.3). Let us also use $\delta(\beta_0^3/\beta_2^3 - 1)$ to eliminate β_0^3 , imposing (3.10). Integrating over β_0^3 gives a factor β_2^3 , so the measure becomes

$$-\beta_2^3 d\beta_2^3 \prod_{\mathbb{A} \neq 4} d\beta_1^{\mathbb{A}} \prod_{k \in \{0,2\}} \prod_{\mathbb{A} \neq 3,4} d\beta_k^{\mathbb{A}}. \quad (3.16)$$

We rewrite this as a measure for the single transverse coordinate β_2^3 , times a measure on \mathcal{M}_{int} , for which a full set of 7|12 coordinates were given in (3.8) and (3.9):

$$-(\beta_2^3)^{1-4} d\beta_2^3 \times \left(\prod_{\mathbb{A} \neq 4} d\beta_1^{\mathbb{A}} \prod_{k \in \{0,2\}} \prod_{\mathbb{A} \neq 3,4} d\left(\frac{\beta_k^{\mathbb{A}}}{\beta_k^3}\right) \right). \quad (3.17)$$

The extra power (-4) in $(\beta_2^3)^{-4}$ was calculated as $2_{k=0,2} \times (2_B - 4_F)$; the terms 2_B and -4_F arise from the redefined bosonic *and* fermionic measures involving $\beta_k^{\mathbb{A}}$, respectively.

The coordinate β_2^3 is related to the deformation parameter C — we will see that the natural definition of C is $(\beta_2^3)^2$. The measure $(\beta_2^3)^{-3} d\beta_2^3$ occurring in (3.17) will be corrected to $d\beta_2^3/\beta_2^3$ — the desired pole — once we include an extra factor $(\beta_2^3)^2$ which comes from the free-fermion correlator ω . We now turn to the analysis of this factor.

3.2.2 Factors from the fermion correlator

The integrand (3.2) contains the factor

$$\omega(\sigma_1, \dots, \sigma_n) = \prod_{i=1}^n \frac{d\sigma_i}{\sigma_i - \sigma_{i+1}}, \quad \sigma_{n+1} \equiv \sigma_1. \quad (3.18)$$

We would like to investigate how this form behaves on conics that are degenerating into a pair of lines (i.e., near \mathcal{M}_{int}). The result will be that along \mathcal{M}_{int} , ω factorizes into a product of two copies of ω defined on the two lines separately (with an extra marked σ on each line at the point of intersection), while transverse to \mathcal{M}_{int} , ω vanishes like $(\beta_2^3)^2$.

As the curve degenerates to a pair of lines, some of the n insertions approach one line and some approach the other. We consider the case where

$$\sigma_1, \dots, \sigma_m \quad (3.19)$$

approach one asymptote while the remaining $(n - m)$ insertions

$$\sigma_{m+1}, \dots, \sigma_n \quad (3.20)$$

approach the other. This is not the most general choice, since the σ_i come with a fixed cyclic ordering which is built into (3.18); our choice is characterized by the fact that as we run through the cyclic ordering we jump from the first line to the second and back only once. We will comment on other possibilities at the end.

With the $GL(2, \mathbb{C})$ gauge-fixing we chose above, as we approach some point of \mathcal{M}_{int} , the coordinates σ_i do not remain finite; one of the lines is $\sigma \rightarrow 0$ while the other line is $\sigma \rightarrow \infty$. So we need to rescale the σ_i to get new coordinates $\hat{\sigma}_i$ on \mathcal{M}_{int} which label the positions of the marked points; we define $\hat{\sigma}_i$ so that $Z^{\mathbb{A}}$ defined in (3.7) remains constant as $\hat{\sigma}_i$ is kept fixed and $\beta_0^3, \beta_2^3 \rightarrow 0$. The correct redefinition is

$$\sigma_i = \left\{ \begin{array}{ll} (\beta_2^3)^{-1} \hat{\sigma}_i & \text{for } i \in \{1, 2, \dots, m\} \\ \beta_0^3 (\hat{\sigma}'_i)^{-1} & \text{for } i \in \{m+1, m+2, \dots, n\} \end{array} \right\}. \tag{3.21}$$

(We use two different symbols $\hat{\sigma}_i$ and $\hat{\sigma}'_i$ to distinguish the coordinates on the two different lines.) Rewriting ω from (3.18) in terms of $\hat{\sigma}_i$ and $\hat{\sigma}'_i$, we obtain

$$\begin{aligned} \omega(\hat{\sigma}_1, \dots, \hat{\sigma}'_n) = & \beta_0^3 \beta_2^3 \left(\prod_{i=1}^{m-1} \frac{d\hat{\sigma}_i}{\hat{\sigma}_i - \hat{\sigma}_{i+1}} \right) \frac{d\hat{\sigma}_m}{\hat{\sigma}_1 \hat{\sigma}_m} \\ & \left(\prod_{i=m+1}^{n-1} \frac{d\hat{\sigma}'_i}{\hat{\sigma}'_i - \hat{\sigma}'_{i+1}} \right) \frac{d\hat{\sigma}'_n}{\hat{\sigma}'_{m+1} \hat{\sigma}'_n} + \dots, \end{aligned} \tag{3.22}$$

where the intersection was defined to be at $\hat{\sigma} = \hat{\sigma}' = 0$. The dots in (3.22) indicate the terms suppressed by powers of $\beta_0^3 \beta_2^3$.

Most of the powers of β_0^3 and β_2^3 have canceled, but there is an extra factor of $\beta_0^3 \beta_2^3$, which equals $(\beta_2^3)^2$ because of our gauge choice (3.10). Also, we obtained the expected free-fermion contractions, including the $2+2$ contractions involving the intersection of the two lines at $\hat{\sigma} = \hat{\sigma}' = 0$.

Note that β_0^3 and β_2^3 always appeared in the combination

$$C = \beta_0^3 \beta_2^3 \tag{3.23}$$

that is invariant under (3.5). This is the same C that we used in figure 5; in fact, one can rewrite our curve in the form

$$xy = C, \tag{3.24}$$

where x, y are coordinates on a plane in $\mathbb{CP}^{3|4}$. The limit $C \rightarrow 0$ describes the singular conics. Note that it is C rather than β_2^3 that is a good coordinate — this is because a simultaneous sign flip on β_0^3 and β_2^3 is the

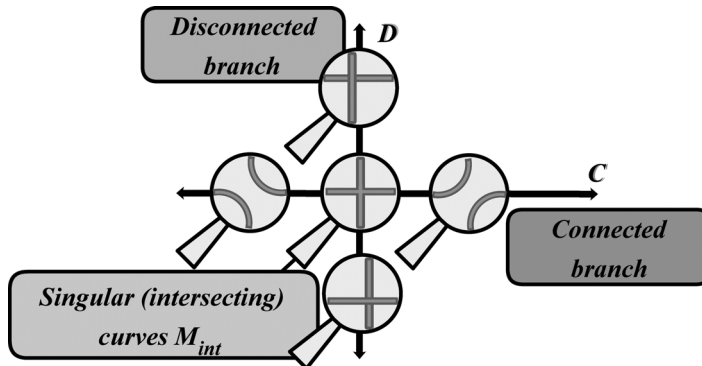


Figure 5: A degenerate configuration of two intersecting lines in $\mathbb{C}\mathbb{P}^{3|4}$ can be deformed into a smooth connected curve of degree 2 or into two disconnected lines. The transition between the two branches of moduli space is reminiscent of a conifold transition.

gauge transformation (3.5) with $\lambda = i$, which preserves our gauge choices (3.10).

Finally, it is easy to check that if we choose a different distribution of the marked points, the result comes out suppressed by additional powers of C . We are only interested in the leading terms, which are linear in C and will give the coefficient of dC/C .

3.3 Finishing the argument in degree 2 case

Now we can collect the results from the previous two subsections. The powers of β_2^3 from (3.17) and (3.22) combine to give $\int d\beta_2^3/\beta_2^3$, which is proportional to $\int dC/C$. So as advertised, integral (3.2) localizes after contour integration to an integral over \mathcal{M}_{int} . The symmetries of $\mathbb{C}\mathbb{P}^{3|4}$ determine the measure for the moduli of the two lines in \mathcal{M}_{int} , which therefore agrees with the measure μ_{int} in (3.1) up to an overall constant; as for the integral over the marked points, comparing (3.22) and (3.1), we see that these measures are also identical. This completes the argument for equivalence in the $d = 2$ case.

Incidentally, one can also compare the measures on \mathcal{M}_{int} directly, without recourse to a symmetry argument. We have already computed the measure which arises from the connected prescription, in (3.17), so the job is to compute the measure μ_{int} which arises from the disconnected prescription. This computation is given (in greater generality) in Section 4.4.

4 Higher degree

Now let us consider the connected prescription for general degree d . We will see that the fully disconnected description and the fully connected prescription are not only equivalent, they are just two extreme cases of a more general class of rules to calculate the amplitude. We will find d a priori different expressions for the scattering amplitude with $d + 1$ negative-helicity gluons,

$$\mathcal{A}_{[K]}, \quad K = 0, 1, 2, \dots, d - 1, \quad (4.1)$$

where $K + 1$ denotes the total number of curves involved in the prescription.¹²

The organization of this section is as follows:

- Section 4.1 outlines the argument that the completely connected and completely disconnected prescriptions agree;
- Section 4.2 discusses the intermediate prescriptions with arbitrary K and their diagrammatic interpretation;
- Section 4.3 generalizes the residue calculation of Section 3.2 to the case of a degree d curve splitting into two curves of degrees d_1 and d_2 ;
- Section 4.4 shows that the residues occurring for any degeneration are actually independent of the chosen prescription, completing the argument.

4.1 The proof in higher degree case

Rather than showing directly that the connected prescription arising from a single connected degree d curve is equivalent to the disconnected prescription involving d lines, we will first show that it is equivalent to a computation involving two disconnected components of degrees d_1, d_2 , such that

$$d_1 + d_2 = d. \quad (4.2)$$

The proof is a generalization of the computation we did in Section 3.2: namely, in Section 4.3, we will find a pole on each boundary divisor $\mathcal{M}_{\text{int}}^\Gamma$, corresponding to a degeneration into intersecting curves,

$$\Sigma_d \longrightarrow \Sigma_{d_1} \cup \Sigma_{d_2}, \quad d_1 + d_2 = d, \quad (4.3)$$

with a particular distribution of the marked points.

¹²Later we will see that K also represents the codimension in moduli space on which the prescription is localized, or equivalently the number of internal propagators which appear in the prescription.

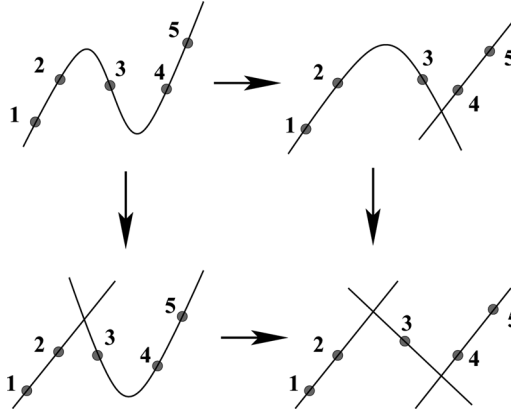


Figure 6: A degeneration of a degree 3 curve into three intersecting lines can be viewed as a two-step process. The moduli space of degree 3 maps with five marked points, $\overline{\mathcal{M}}_{0,5,3}$, contains divisors, $\mathcal{M}_{\text{int}}^{\Lambda_1}$ and $\mathcal{M}_{\text{int}}^{\Lambda_2}$, associated with degenerations into a degree 2 curve and a line shown at the intermediate stages. The moduli space $\mathcal{M}_{\text{int}}^{\Gamma}$ of three intersecting lines (shown in the lower right corner) can be identified with the intersection $\mathcal{M}_{\text{int}}^{\Lambda_1} \cap \mathcal{M}_{\text{int}}^{\Lambda_2}$.

Next we want to show iteratively that this integral over curves with 2 irreducible components is equivalent to one over curves with three components, and so on until eventually we reach d components (all of which must have degree 1). The idea which makes this iteration possible is the following: consider some locus $\mathcal{M}_{\text{int}}^{\Gamma}$, corresponding to a particular degeneration of Σ into $K+1$ components, with a particular distribution of the marked points. This locus can be obtained as an intersection of K boundary divisors, $\mathcal{M}_{\text{int}}^{\Lambda_j}$, each of which is associated with a degeneration of Σ_d into two irreducible components,¹³

$$\mathcal{M}_{\text{int}}^{\Gamma} = \mathcal{M}_{\text{int}}^{\Lambda_1} \cap \dots \cap \mathcal{M}_{\text{int}}^{\Lambda_K}. \quad (4.4)$$

An example is shown in figure 6. In this sense, the problem of studying a general degeneration boils down to understanding the basic process (4.3).

So let us start with the integral over K -component curves and try to prove that it agrees with an integral over $(K+1)$ -component curves. In the K -component case, we have to integrate over various loci $\mathcal{M}_{\text{int}}^{\Gamma}$ as in (4.4). Since the various divisors $\mathcal{M}_{\text{int}}^{\Lambda}$ meet transversally [16], in integrating over each such $\mathcal{M}_{\text{int}}^{\Gamma}$ we will encounter poles wherever $\mathcal{M}_{\text{int}}^{\Gamma}$ intersects another

¹³We use Γ to denote a general degeneration into $K+1$ components and Λ to denote a degeneration into just two components.

divisor $\mathcal{M}_{\text{int}}^\Lambda$.¹⁴ We choose our contour so that it picks up the residues at these poles. In this way, we reduce the integral over $\mathcal{M}_{\text{int}}^\Gamma$ to the sum of integrals over all intersections $\mathcal{M}_{\text{int}}^\Gamma \cap \mathcal{M}_{\text{int}}^\Lambda$. Then we have to sum over all Γ describing K -component degenerations. What is the result of all this summation? From the perspective of the $(K+1)$ -component degenerations — which we label by Γ' — the answer is clear: given some

$$\mathcal{M}_{\text{int}}^{\Gamma'} = \mathcal{M}_{\text{int}}^{\Lambda_1} \cap \cdots \cap \mathcal{M}_{\text{int}}^{\Lambda_K}, \quad (4.6)$$

there are K ways to make it by intersecting some $\mathcal{M}_{\text{int}}^\Gamma$ with some $\mathcal{M}_{\text{int}}^{\Lambda_i}$. Therefore, we get a sum over all $(K+1)$ -component degenerations, with an *overall* multiplicative factor K .

Finally, after repeating this process $d-1$ times, we arrive at an integral over the moduli space of connected trees consisting of d lines, with all possible shapes for the tree and all allowed distributions of marked points. But the arguments of [7] show that the disconnected prescription also reduces to such an integral, by a similar process of localization to poles. Furthermore, in Section 4.3, we will see that the residues in these two computations agree; this will complete the proof.

4.2 Intermediate prescriptions

In Section 4.1, we encountered $d-1$ different moduli spaces $\mathcal{M}_{\text{int}}^K$ of singular curves, characterized by the number $K+1$ of components, which interpolated between the non-singular degree d curve ($K=0$) and the tree of degree 1 curves ($K=d-1$). Furthermore, we obtained integrals over each $\mathcal{M}_{\text{int}}^K$ by starting with the connected prescription ($K=0$) and successively localizing to poles. As a result of this localization all these integrals are equal; now we want to argue that the intermediate cases $K=1, \dots, d-2$ can be naturally interpreted as coming from “intermediate prescriptions,” involving integrals over the moduli of $K+1$ disconnected curves with K propagators connecting them. We defined these prescriptions at the end of Section 2.2.

The argument is a generalization of the “heuristic” derivation of the computational rules for the disconnected prescription, given in [7]. Namely,

¹⁴One way to understand this is to note that if we start with the full $\overline{\mathcal{M}}_{0,n,d}$ and look near such an intersection of K divisors, the integrand looks like

$$\frac{dC_1}{C_1} \wedge \cdots \wedge \frac{dC_K}{C_K} \wedge (\text{regular}). \quad (4.5)$$

We have already contour-integrated over C_1, \dots, C_{K-1} and thus restricted to $C_1 = \cdots = C_{K-1} = 0$, i.e., to $\mathcal{M}_{\text{int}}^\Gamma$; after doing this, we get simply dC_K/C_K , with a pole at $C_K = 0$, i.e., at $\mathcal{M}_{\text{int}}^\Gamma \cap \mathcal{M}_{\text{int}}^\Lambda$.

starting from the intermediate prescription, note that the propagator $D(\cdot, \cdot)$ by definition satisfies

$$\bar{\partial}D = \Delta. \quad (4.7)$$

Here Δ is a $(0, 3)$ -form on $(\mathbb{CP}^{3|4})^2$ which is concentrated on the diagonal $\mathbb{CP}^{3|4}$; in inhomogeneous coordinates with $Z^4 = Z'^4 = 1$, it may be written

$$\Delta = \bar{\delta}(Z^1 - Z'^1) \bar{\delta}(Z^2 - Z'^2) \bar{\delta}(Z^3 - Z'^3) \delta^4(\psi - \psi'), \quad \bar{\delta}(f) := \delta^2(f) d\bar{f}. \quad (4.8)$$

Equation (4.7) means that $D(\cdot, \cdot)$ is meromorphic with a pole along the diagonal. The integral over $\mathcal{M}_{\text{int}}^K$ in the disconnected prescription contains K propagators (2.16); these factors therefore have poles when $Q_i(\sigma) = Q_{i'}(\sigma')$.

As in [7], we assume that K of the integrals over moduli of the disconnected curves are evaluated on contours which encircle these poles, in a suitable sense. Using (4.7), performing these contour integrals is equivalent to filling in the contour and replacing D by Δ . This localizes the integral to the sublocus of moduli space where all propagators have shrunk to zero length, which is exactly $\mathcal{M}_{\text{int}}^K$.

So finally we have d different prescriptions, involving summing over configurations with 1 curve (connected case), 2, 3, \dots , d curves (maximally disconnected case), and we have argued that each of these prescriptions is equivalent, up to an overall rescaling. In this sense, any of them can be used to calculate the Yang–Mills amplitudes.

Of course, another possibility is that the correct amplitudes are obtained by summing different contributions from various sorts of diagrams with various numbers of curves. We have argued that all such contributions are proportional to one another, so such a modified rule would only change the overall prefactor. Although we will not try to make the final verdict in this paper, we believe that a more detailed analysis of the prescriptions (including the coefficients) should be able to resolve this uncertainty.

4.2.1 Diagrammatic interpretation and an example

Now let us discuss the diagrammatic interpretation of the intermediate prescriptions. We have seen that the K th intermediate prescription is naturally localized on $\mathcal{M}_{\text{int}}^K$, which is a union of various $\mathcal{M}_{\text{int}}^\Gamma$. Here Γ describes the decomposition of the curve Σ_d into $K + 1$ components and the distribution of marked points along these components. Equivalently, we could say that Γ describes a slight generalization of an MHV tree diagram: namely, it is a tree diagram with $K + 1$ vertices, where each vertex now carries an internal index d_i , subject to the rule that $\sum d_i = d$. The MHV diagrams are the case where all $d_i = 1$.

It would be very useful if we could give a compact formula for the contribution of a general vertex with arbitrary d_i , analogous to the off-shell continuation of the MHV amplitude given in [7]. At the moment, we do not possess such a formula, so we can only define the diagram Γ to be the integral over $\mathcal{M}_{\text{int}}^\Gamma$ which we considered above. In this language, our localization argument relating different prescriptions becomes the statement that the contribution from a diagram Γ agrees with the sum over all Γ' obtained by “splitting a vertex” in Γ . In other words, Γ' should be obtained by replacing a vertex with index d by a pair of vertices with indices d_1, d_2 , such that $d_1 + d_2 = d$, with a propagator connecting them. This is the diagrammatic analog of a degree d curve which degenerates into two curves with degrees d_1, d_2 .

We can also repeat the combinatorics from Section 4.1 in this language. Start with a diagram with $K+1$ vertices. This diagram contains K propagators. Therefore there are K ways to shrink a single propagator and obtain a “parent” diagram with K vertices. Because a diagram with $K+1$ vertices has K parents, the sum over the daughters with $K+1$ vertices equals K times the sum over the parents with K vertices.

To illustrate how all this works when external wave functions of fixed helicity are included, let us consider a 6-gluon amplitude $\mathcal{A}_{[+--+---]}$. If we were to use the connected prescription, we would have to integrate over the moduli space $\overline{\mathcal{M}}_{0,6,3}$ of degree 3 curves. On the other hand, in the disconnected prescription, one has to consider three degree 1 curves, which can be interpreted as MHV vertices in Yang–Mills theory [7]. Therefore, in this case, one has to sum over all tree graphs with three MHV vertices connected by Yang–Mills propagators (figure 7). In total, there are 19 such graphs contributing to $\mathcal{A}_{[+--+---]}$.

Now let us consider the intermediate prescription with $K = 1$. This prescription leads to a sum over tree graphs with two vertices, one MHV and one non-MHV (the non-MHV vertex involves three insertions of negative helicity). Examples of such graphs with non-MHV vertices are shown in

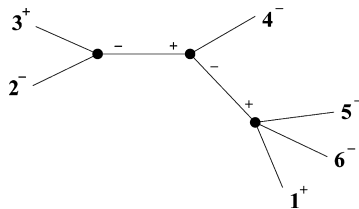


Figure 7: An MHV tree diagram contributing to $\mathcal{A}_{[+--+---]}$.

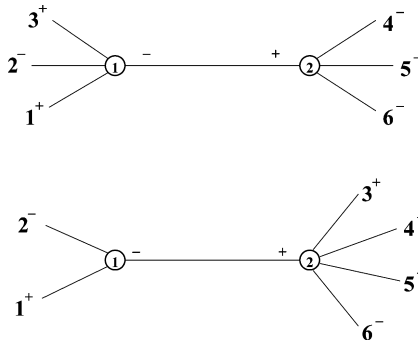


Figure 8: Two types of tree diagram with one MHV and one non-MHV (degree 2) vertex that contribute to the $\mathcal{A}_{[+--+---]}$ amplitude. In total, there are six diagrams of each kind. The number attached to each vertex represents the degree of the corresponding curve in twistor space.

figure 8. There are 12 such diagrams which contribute to $\mathcal{A}_{[+--+---]}$. Since each non-MHV vertex itself can be represented as a sum over tree diagrams with two MHV vertices, we should be able to reproduce the disconnected prescription if we split all non-MHV vertices into MHV ones. More precisely, in this decomposition we should encounter each MHV diagram twice (since in the disconnected prescription $K = 2$). Indeed, it is straightforward to check that the 12 non-MHV diagrams lead to 38 MHV graphs, in agreement with the general rule.

4.3 Computing the residue in higher degree case

Returning from our digression to discuss the intermediate prescriptions, in this section, we show that integral (2.9) over the moduli space $\overline{\mathcal{M}}_{0,n,d}$ which arises in the connected prescription has a pole along the codimension 1 divisor $\mathcal{M}_{\text{int}}^1$ describing curves that are degenerated into two components. We further verify that the residue is the same as that which arises after localization of the $K = 1$ prescription on $\mathcal{M}_{\text{int}}^1$, thus establishing the equivalence between connected and $K = 1$ prescriptions.

We want to study a degeneration in which the curve Σ_d degenerates into a pair of intersecting curves, Σ_{d_1} and Σ_{d_2} , of degree d_1 and d_2 , as in (4.3). Using the projective symmetry to divide by σ^{d_1} , we can write the degree d map (2.2) as

$$Z^{\mathbb{A}}(\sigma) = \sum_{k=-d_1}^{d_2} \beta_{d_1+k}^{\mathbb{A}} \sigma^k. \quad (4.9)$$

We fix the $GL(2, \mathbb{C})$ symmetry similarly to the degree 2 case, namely by conditions based on (3.3) and (3.10):

$$(\beta_{d_1-1}^4, \beta_{d_1}^4, \beta_{d_1+1}^4) = (0, 1, 0), \quad \frac{\beta_{d_1-1}^3}{\beta_{d_1+1}^3} = 1, \tag{4.10}$$

and define the deformation parameter $C := \beta_{d_1-1}^3 \beta_{d_1+1}^3$. As in degree 2, the singular limit will be $C \rightarrow 0$, or equivalently $\beta_{d_1+1}^3 \rightarrow 0$, and the question is how the other coefficients should scale in this limit.

The correct scaling is as follows: we take $\beta_{d_1-1}^3 = \beta_{d_1+1}^3 \rightarrow 0$ while holding finite the quantities

$$\alpha_k^{\mathbb{A}} := \frac{\beta_{d_1-k}^{\mathbb{A}}}{(\beta_{d_1-1}^3)^k}, \quad 0 \leq k \leq d_1; \quad \alpha_k'^{\mathbb{A}} := \frac{\beta_{d_1+k}^{\mathbb{A}}}{(\beta_{d_1+1}^3)^k}, \quad 0 \leq k \leq d_2. \tag{4.11}$$

In that limit we obtain two curves,

$$\begin{aligned} \Sigma_{d_1}: Z^{\mathbb{A}}(\hat{\sigma}) &= \sum_{k=0}^{d_1} \alpha_k^{\mathbb{A}} \hat{\sigma}^k, \\ \Sigma_{d_2}: Z^{\mathbb{A}}(\hat{\sigma}') &= \sum_{k=0}^{d_2} \alpha_k'^{\mathbb{A}} \hat{\sigma}'^k. \end{aligned} \tag{4.12}$$

Namely, we obtain the points $Z^{\mathbb{A}}(\hat{\sigma})$ on Σ_{d_1} by holding fixed $\hat{\sigma} = \sigma/\beta_{d_1-1}^3$ in the limit, and we obtain the points $Z^{\mathbb{A}}(\hat{\sigma}')$ on Σ_{d_2} by holding fixed $\hat{\sigma}' = \sigma\beta_{d_1+1}^3$ in the same limit (figure 9).

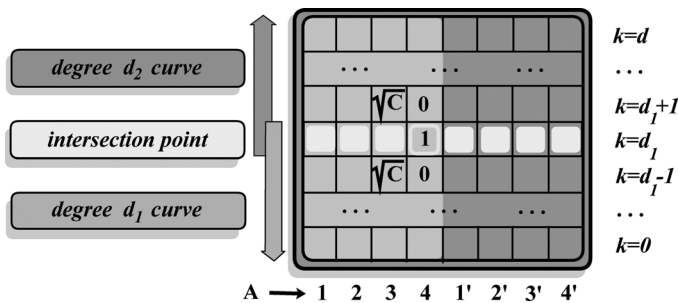


Figure 9: The organization of the coefficients $\beta_k^{\mathbb{A}}$ for a degree d curve degenerating into curves of degrees d_1 and d_2 . The symmetry $GL(2, \mathbb{C})$ is fixed by setting three bosonic coefficients to the values $(0, 1, 0)$ and two others to \sqrt{C} ; this C is the deformation parameter, which approaches zero in the degeneration limit.

Therefore the parameters $\alpha_k^{\mathbb{A}}, \alpha'_k{}^{\mathbb{A}}$ give coordinates on $\mathcal{M}_{\text{int}}^1$, specifying the moduli of the degenerated curve. (Note that $\alpha_0^{\mathbb{A}} = \alpha'_0{}^{\mathbb{A}}$; these shared coordinates specify the intersection point of Σ_{d_1} and Σ_{d_2} .)

Now we want to study how our integral (2.9) behaves near $\mathcal{M}_{\text{int}}^1$. As in Section 3.2, we have to compute the Jacobian J from the gauge-fixing of $GL(2, \mathbb{C})$. The matrix of variations generalizing (3.13) is

$$\delta \begin{pmatrix} \beta_{d_1-1}^4 \\ \beta_{d_1}^4 \\ \beta_{d_1+1}^4 \\ \beta_{d_1-1}^3 / \beta_{d_1+1}^3 \end{pmatrix} = \begin{pmatrix} d_2 & (d_1 + 2)\beta_{d_1+2}^4 & 0 & 0 \\ d_2 + 2)\beta_{d_1-2}^4 & d_1 & 0 & 0 \\ 0 & 0 & d_1 & d_2 \\ * & * & 2 & -2 \end{pmatrix} \begin{pmatrix} b \\ c \\ a \\ d \end{pmatrix}. \tag{4.13}$$

In the singular limit, the $\beta_{d_1\pm 2}^4$ terms in (4.13) vanish, and we get

$$J \rightarrow -2d_1d_2d. \tag{4.14}$$

The gauge-fixed integral includes the factor $J/2d$; the $2d$ comes from an unfixed subgroup of $GL(2, \mathbb{C})$, analogous to (3.15), which is $\mathbb{Z}_2 \times \mathbb{Z}_d$ if both d_1 and d_2 are even and \mathbb{Z}_{2d} otherwise. Next we have to rewrite the integrand in terms of the new coordinates (4.11). One might be worried that switching to these coordinates will generate extra powers of C beyond what we had in the degree 2 case, spoiling the conclusion that there is a pole along $\mathcal{M}_{\text{int}}^1$. But this does not occur; if we increase d_1 by 1, for example, the integrand just acquires an extra integral over 4|4 variables:

$$\mu \rightarrow \mu \wedge \prod_{\mathbb{A}} d\beta_0^{\mathbb{A}} = \mu \wedge \prod_{\mathbb{A}} d\alpha_{d_1}^{\mathbb{A}} \tag{4.15}$$

The powers of $\beta_{d_1+1}^3$ simply cancel between the four bosons and four fermions! Unlike the coefficients $\beta_{d_1}^{\mathbb{A}}$ and $\beta_{d_1\pm 1}^{\mathbb{A}}$, among which five special bosonic components have been used to gauge-fix the $GL(2, \mathbb{C})$ symmetry or to describe the parameter C , the additional moduli $\beta_{d_1\pm k}^{\mathbb{A}}$ with $k > 1$ come in full “supermultiplets” containing four bosons and four fermions. Therefore no new powers of C are generated in rescaling β ’s to α ’s, so the measure for the moduli of the degenerating curve still behaves as dC/C^2 near $C = 0$. Similarly, the free-fermion correlator ω factorizes,

$$\omega(\sigma) \rightarrow C \omega_1(\hat{\sigma}) \wedge \omega_2(\hat{\sigma}'), \tag{4.16}$$

just as in degree 2.

So we have a pole along $\mathcal{M}_{\text{int}}^1$, as in the degree 2 case, and after integrating around this pole, the fully gauge-fixed measure for the moduli of the

degenerate curve is

$$-d_1 d_2 \prod_{\mathbb{A}} \left(\prod'_{k=0}^{d_1} d\alpha_k^{\mathbb{A}} \prod'_{k=1}^{d_2} d\alpha_k'^{\mathbb{A}} \right). \tag{4.17}$$

Here the symbol \prod' indicates that we omit the five factors

$$d\alpha_1^4, \quad d\alpha_1'^4, \quad d\alpha_0^4, \quad d\alpha_1^3, \quad d\alpha_1'^3; \tag{4.18}$$

there are no such α 's among the coordinates on $\mathcal{M}_{\text{int}}^1$, because their corresponding β 's were used up in the gauge-fixing and in the transverse coordinate C , as shown in figure 9.

4.4 Finishing the argument in higher degree case

Finally we have to check that measure (4.17) agrees with the one coming from localization of the $K = 1$ prescription. From Section 4.2, we know that the latter measure is obtained as follows: start with two curves of degree d_1, d_2 ,

$$\begin{aligned} Q^{\mathbb{A}}(\sigma) &= \sum_{k=0}^{d_1} \alpha_k^{\mathbb{A}} \sigma^k, \\ Q'^{\mathbb{A}}(\sigma') &= \sum_{k=0}^{d_2} \alpha_k'^{\mathbb{A}} \sigma'^k. \end{aligned} \tag{4.19}$$

(The notation $\alpha_k^{\mathbb{A}}, \alpha_k'^{\mathbb{A}}$ we use here agrees with the notation we used above for the moduli of the curves obtained by a degeneration; compare (4.19) with (4.12) and (4.11). The only difference is that here we do not necessarily have $\alpha_0^{\mathbb{A}} = \alpha_0'^{\mathbb{A}}$). Then we have the standard measure (2.3) on the two curves separately, which before gauge-fixing is

$$\mu_{d_1} \wedge \mu_{d_2} = \prod_{\mathbb{A}} \left(\prod_{k=0}^{d_1} d\alpha_k^{\mathbb{A}} \prod_{k=0}^{d_2} d\alpha_k'^{\mathbb{A}} \right). \tag{4.20}$$

As explained in Section 4.2, the requirement that the two curves actually intersect is enforced by a delta function which is coupled to one marked point on each curve,

$$\Delta(Q(\sigma), Q'(\sigma')). \tag{4.21}$$

To compare the measures (including this delta function), we have to gauge-fix the $GL(2, \mathbb{C})^2$ symmetry acting on the coefficients $\alpha_k^{\mathbb{A}}, \alpha_k'^{\mathbb{A}}$. There are many ways to do this; we choose a way that is as similar as possible to

the gauge-fixing we used for the degenerating degree d curve, so that the unfixed moduli will match directly. Namely, we take

$$\alpha_0^i = \alpha_0'^i \text{ for } i \in \{2, 3\}, \quad (4.22)$$

$$\alpha_0^4 = \alpha_0'^4 = 1, \quad (4.23)$$

$$\alpha_1^4 = \alpha_1'^4 = 0, \quad (4.24)$$

$$\alpha_1^3 = \alpha_1'^3 = 1. \quad (4.25)$$

The matrix of variations from this gauge-fixing is similar to (4.13), but since it is an 8×8 matrix we just write the answer here:

$$J = (d_1 d_2)^2 (\alpha_1^2 - \alpha_1'^2). \quad (4.26)$$

The gauge-fixing factor is $J/d_1 d_2$, because of the subgroup $\mathbb{Z}_{d_1} \times \mathbb{Z}_{d_2} \subset GL(2, \mathbb{C}) \times GL(2, \mathbb{C})$, roots of unity acting on each curve separately; since this subgroup acts trivially, it is unfixed by our gauge condition. Next we must include the integral over the delta function (4.21), which we write as

$$\int d\sigma d\sigma' \delta^{(3|4)} \left(\frac{Q^\mathbb{A}(\sigma)}{Q^4(\sigma)} - \frac{Q'^\mathbb{A}(\sigma')}{Q'^4(\sigma')} \right). \quad (4.27)$$

With our gauge choice, it is easy to study the behavior of this delta function in the vicinity of $\sigma = \sigma' = 0$.¹⁵ One uses the Z^2 and Z^3 components of the delta function to set $\sigma = \sigma' = 0$, obtaining

$$\frac{1}{(\alpha_1^2 - \alpha_1'^2)} \delta(\alpha_0^1 - \alpha_0'^1) \prod_{\mathbb{A}=1'}^{4'} \delta(\alpha_0^\mathbb{A} - \alpha_0'^\mathbb{A}). \quad (4.28)$$

Note that the 1|4 delta functions in (4.28), combined with the gauge conditions (4.22) and (4.23), are enough to set all $\alpha_0'^\mathbb{A} = \alpha_0^\mathbb{A}$. This was the main motivation for this gauge-fixing; the point $\alpha_0^\mathbb{A}$ represents the intersection of the two curves and the remaining moduli are precisely the ones we had for the degenerating degree d curve in (4.17). Therefore we easily see that the measures agree, including the prefactor $d_1 d_2$. (Although we have not been careful about overall constant factors, the absence of a relative factor here is important — it corresponds to the absence of prefactors weighing different diagrams in the intermediate prescriptions).

This completes the argument for the equivalence between the connected and $K = 1$ prescriptions. It also sets up the iteration we described in

¹⁵Although our gauge choice was rigged so that studying $\sigma = \sigma' = 0$ would recover the desired moduli space of intersecting curves, it is not clear a priori from our arguments why one should consider only this region; this is related to the issue of the exact contour choice in the intermediate prescription, which we will not settle here. We are also integrating over the delta function as if it were real instead of holomorphic; similar manipulations were used in [10].

Section 4.1 to prove the equivalence of all prescriptions, by successive localization to poles in higher and higher codimension, corresponding to more and more degenerate curves.

One detail remains: we have to check that the residues we obtain are always independent of which prescription we started with. In other words, we have to prove that the measure for the integral over $K + 1$ -component trees obtained by some degeneration process always agrees with the measure coming from the disconnected prescription. As we know from Section 4.2, the latter measure can be written as a product of measures for the individual curves, with delta functions that guarantee the curves intersect. We just proved the agreement for $K = 1$. For general K we can work inductively; given a $K + 1$ -component tree on which some curve is further degenerating, just focus on the measure for that curve, and note that the delta functions from the other curves are well behaved on moduli space near the degeneration we are studying. In this sense, the degenerating curve can be isolated from the rest of the tree. The computation done above in the $K = 1$ case then shows that the measure after this degeneration agrees with that from the disconnected prescription. This then completes the argument for the equivalence of all prescriptions.

5 Conclusions and open questions

We have argued for the equivalence of the connected and disconnected twistorial formulae for the tree-level scattering amplitudes of $\mathcal{N} = 4$ super Yang–Mills, provided that the contours are appropriately chosen. Using this equivalence, we can now exploit the complementary virtues of the two prescriptions simultaneously. As we remarked in the introduction, the connected prescription minimizes the number of diagrams one has to sum, namely, there is only one; the amplitude is expressed as a single integral, which was the starting point for several theoretical developments [8–10]. The disconnected prescription involves more diagrams, but still a manageable number for some interesting amplitudes, and the contribution from each diagram can be immediately written down.

To conclude, we summarize some of the many remaining open problems in this area:

- **Contours I.** Is there a rigorous justification of the choice of contours in all these calculations? In our argument for the equivalence between connected and disconnected prescriptions, we identified specific poles in the integral over moduli, and we roughly wanted a contour which

encircles all of these poles. We believe it should be possible to show by a deformation argument that our choice of contour is equivalent to the one used in [6], thus completing the proof of equivalence, but this seems to be non-trivial; the computations in [6] depend on a particular method of evaluating the integral in the connected prescription by saturating delta functions, and it is difficult to see which contour it corresponds to.

- **Contours II.** Once the residues are isolated in both prescriptions, we must still integrate over the degeneration locus \mathcal{M}_{int} , which requires yet another choice of contour; for example, the integration over t from 0 to ∞ in Section 6 of [7] should have some a priori justification. This paper has not addressed this question. Our argument for the equivalence requires that the contours on \mathcal{M}_{int} are chosen to be equivalent in all prescriptions.
- **Explicit external wave functions.** Our derivation was rather formal. It did not depend on the particular form of the wave functions. Of course, it would be interesting to verify the picture by calculating the amplitudes involving particles with well-defined momenta, i.e., $(\lambda, \tilde{\lambda}, \psi)$ using our generalized prescriptions. Unlike the MHV vertices in [7], one might expect that the $d > 1$ vertices will be ratios of polynomials involving both λ and $\tilde{\lambda}$. (Of course, it is also possible that one will not obtain any compact formula for the $d > 1$ vertices in this way).
- **Derivation from the B-model.** Both connected and disconnected contributions seem to arise in the topological B-model of [1] as long as we use not only the degree d D1-instantons but also the propagators (and vertices) of the holomorphic Chern–Simons theory. Does our equivalence suggest that the D1-instantons are not independent of the Chern–Simons degrees of freedom?
- **Real versions.** The framework first proposed by Berkovits [8] and the topological A-model of [15] seem to prefer the real version of the twistor space, $\mathbb{RP}^{3|4}$, and correspondingly real values of the moduli. Is there a real variation of our procedures? One can imagine that the disconnected rules for the amplitudes might be derived from the cubic twistorial string field theory of [9] if K stringy propagators are expanded in component fields, so that the different parts of the world-sheet become effectively disconnected.
- **Choice of prescriptions.** According to our analysis, there is significant freedom to choose a twistor prescription for tree diagrams; we gave d different rules, all of which agree up to overall prefactors. Is this all one can say, or would a more sensitive study give more information about which is the “correct” prescription? Does this proliferation of prescriptions persist beyond tree level?

- **Loops and higher genus.** We only studied tree diagrams, corresponding to genus zero curves. What are the exact rules and equivalences between various formulae for loop and non-planar amplitudes? Our analysis suggests that an investigation of possible degenerations of genus g curves should be relevant for the understanding of loop diagrams in the twistor string.

Acknowledgments

We are grateful to Michal Fabinger, Peter Svrček, Cumrun Vafa, Anastasia Volovich, and Edward Witten for very useful discussions. This work was conducted during the period S.G. served as a Clay Mathematics Institute Long-Term Prize Fellow. S.G. is also supported in part by RFBR grant 01-02-17488. The work of L.M. was supported in part by Harvard DOE grant DE-FG01-91ER40654 and the Harvard Society of Fellows. The work of A.N. was supported by NSF grants PHY-0255841 and DMS-0244464.

References

- [1] E. Witten, *Perturbative gauge theory as a string theory in twistor space*, [hep-th/0312171](#).
- [2] S.J. Parke and T.R. Taylor, *An amplitude for n gluon scattering*, *Phys. Rev. Lett.* **56** (1986), 2459.
- [3] M.L. Mangano, S.J. Parke and Z. Xu, *Duality and multi-gluon scattering*, *Nucl. Phys.* **B298** (1988), 653.
- [4] R. Roiban, M. Spradlin and A. Volovich, *A googly amplitude from the B -model in twistor space*, [hep-th/0402016](#).
- [5] R. Roiban and A. Volovich, *All googly amplitudes from the B -model in twistor space*, [hep-th/0402121](#).
- [6] R. Roiban, M. Spradlin and A. Volovich, *On the tree-level S -matrix of Yang–Mills theory*, [hep-th/0403190](#).
- [7] F.A. Cachazo, P. Svrcek and E. Witten, *MHV vertices and tree amplitudes in gauge theory*, [hep-th/0403047](#).
- [8] N. Berkovits, *An alternative string theory in twistor space for $\mathcal{N} = 4$ super-Yang–Mills*, [hep-th/0402045](#).
- [9] N. Berkovits and L. Motl, *Cubic twistorial string field theory*, [hep-th/0403187](#).
- [10] E. Witten, *Parity invariance for strings in twistor space*, [hep-th/0403199](#).

- [11] C.-J. Zhu, *The googly amplitudes in gauge theory*, hep-th/0403115.
- [12] G. Georgiou and V.V. Khoze, *Tree amplitudes in gauge theory as scalar MHV diagrams*, hep-th/0404072.
- [13] M. Aganagic and C. Vafa, *Mirror symmetry and supermanifolds*, hep-th/0403192.
- [14] N.A. Nekrasov, H. Ooguri and C. Vafa, *S-duality and topological strings*, hep-th/0403167.
- [15] A. Neitzke and C. Vafa, *$\mathcal{N} = 2$ strings and the twistorial Calabi–Yau*, hep-th/0402128.
- [16] W. Fulton and R. Pandharipande, *Notes on stable maps and quantum cohomology*, in Algebraic Geometry — Santa Cruz 1995, Proc. Sympos. Pure Math., Vol. 62, American Mathematical Society, Providence, RI, 1997, 45–96, alg-geom/9608011.

